Journal of Achievements in Materials and Manufacturing Engineering
International Scientific Journal published monthly by the World Academy of Materials and Manufacturing Engineering

The influence of the distribution of non-metalic inclusion on the fatigue strength coefficient of high purity steels

T. Lipiński*
University of Warmia and Mazury in Olsztyn, Faculty of Technical Sciences,
ul. Oczapowskiego 11, 10-957 Olsztyn, Poland
* Corresponding e-mail address: tomekl@uwm.edu.pl

ABSTRACT

Purpose: In this study, attempts were made to analyze the impact of impurities with various diameters and spacing between non-metalic inclusion λ on fatigue strength coefficient k determined under rotary bending fatigue conditions z_{go} of high purity steels produced in an industrial plant.

Design/methodology/approach: The study was performed on 21 heats produced in an industrial plant. Fourteen heats were produced in 140 ton electric furnaces, and 7 heats were performed in a 100 ton oxygen converter. The experimental variants were compared in view of the applied melting technology and heat treatment options. The results were presented to account for the correlations between the fatigue strength coefficient during rotary bending, the diameter of and spacing between submicroscopic impurities.

Findings: Equations for calculating the fatigue strength coefficient at each tempering temperature and a general equation for all tempering temperatures were proposed. Equations for estimating the fatigue strength coefficient based on the relative volume of submicroscopic non-metallic inclusions were also presented. The relationship between the fatigue strength and hardness of high-grade steel vs. the quotient of the diameter of impurities and the spacing between impurities, and the fatigue strength and hardness of steel vs. the relative volume of non-metallic impurities were determined.

Practical implications: The proposed linear regression equations supported the determination of fatigue strength coefficient k and bending fatigue strength as a function of hardness taking into account impurities.

Originality/value: The proposed equations contributes to the existing knowledge base of practices impact of impurities with various diameters and spacing between non-metalic inclusion on fatigue strength.

Keywords: Metallic alloys; Fatigue; Mechanical; Heat treatment

Reference to this paper should be given in the following way:

T. Lipiński, The influence of the distribution of non-metalic inclusion on the fatigue strength coefficient of high purity steels, Journal of Achievements in Materials and Manufacturing Engineering 69/1 (2015) 18-25.

PROPERTIES

1. Introduction

Many working elements in machines and devices are subjected to varied loads during operation. Loading paths can be random, but also cyclic. Load produces complex stress in a material. The selection of steel types that are optimal for a given application contributes to reliable machine operation.

The impurity content is also a key determinant of the quality of high-grade steel. Inclusions may also play an important role, subject to their type and shape. Inclusions may increase the strength of steel by inhibiting the development of micro-cracks. Yet as regards steel, non-metallic inclusions have mostly a negative effect which is dependent on their content, size, shape and distribution [1-3]. The mechanical properties and fatigue strength of structural materials should also be evaluated in view of crystallization conditions [4-8], the manufacturing process [9-12], microstructure [13,14], microsegregation [15-19] and the existing defects [20].

The distribution of inclusions is an equally important factor. Single inclusions and clusters of inclusions exert different effects. Large, individual inclusions can produce discontinuities that grow rapidly under variable load. The clusters of microparticles of a subcritical size lower stress and increase the number of sample-damaging cycles [21-23].

Non-metallic inclusions are one of the factors that influence the fatigue strength of steel. Although steel has a relatively small number of non-metallic inclusions, those impurities have a considerable impact on the material's technological and strength parameters, in particular fatigue strength and life. The presence of oxygen and non-metallic inclusions in steel is a natural consequences of physical and chemical processes during production. The shape of non-metallic inclusions may vary. Spheroidal inclusions are characteristic of steel which contains high levels of oxygen. The addition of small amounts of aluminum leads to partial deoxydation of steel and the formation of inclusions along the boundaries of austenite grains. Excessive amounts of powerful deoxidants contribute to the formation of large faceted inclusions [20].

The quantity of non-metallic inclusions in steel is relatively low, nevertheless, they have a significant impact on the structure, technological and strength parameters of the resulting alloy. The effect of impurities is closely related to the processes taking place in micro-areas, which is why the size of inclusion particles significantly influences the properties of construction materials [24-25].

Alloys subjected to variable loads require high-grade steels. Their properties are determined during complex tests that are costly and time consuming. For this reason, analyses that support quick determination of the evaluated properties are often used in industrial practice. Fatigue strength is one of the evaluated properties of steel. Various functions, nomograms and coefficients are given in the literature for estimating fatigue strength as a function of tensile strength [26] (1).

$$z_g = f(R_m) \tag{1}$$

Various functions are also used to convert fatigue strength for a known load cycle, usually rotary bending, into fatigue strength for a different load cycle, such as one-sided bending based on the results of rotary bending (2).

$$z_{gj} = f(z_{go}) \tag{2}$$

Those relationships are presented for different groups of materials, production processes, heat processing methods, etc. They include other sensitivity coefficients such as the coefficient of material's sensitivity to cycle asymmetry, load type, etc. The presented analytical relations are expressed by the influence coefficient c which is written as follows in equation (3) when ultimate tensile strength R_m is taken into account:

$$z_g = cR_m \tag{3}$$

therefore:

$$c = \frac{z_g}{R_m} \tag{4}$$

Coefficient c is the quotient of fatigue strength z_g divided by tensile strength R_m at static load. To estimate tensile strength based on the results of non-destructive tests, coefficient p was introduced in equation (5) to determine tensile strength as a function of hardness.

$$R_m = pHV \tag{5}$$

Equations (4) and (5) were combined to produce formula (6).

$$c = \frac{z_g}{pHV} \tag{6}$$

Coefficients c and p were substituted with coefficient k to convert equation (6) to (7).

$$k = \frac{z_g}{HV} \tag{7}$$

Equation (4) does not account for steel purity. For this reason, coefficient c can take on a broad range of values. For steel samples subjected to rotary bending, it ranges from 0.36 to 0.6 of tensile strength R_m [27].

The influence of impurities on fatigue strength has been researched extensively, but very few studies analyze the effect of impurities on the coefficient given by equation (7) which is used to estimate fatigue strength based on hardness, i.e. in non-destructive tests. Coefficient k is the quotient of fatigue strength z_g divided by Vickers hardness HV.

In this study, attempts were made to analyze the impact of impurities with various diameters and spacing between non-metalic inclusion λ on fatigue strength coefficient k determined under rotary bending fatigue strength z_{go} of high purity steels produced in an industrial plant.

3. Methods

The study was carried out in an industrial setting with the aim of reproducing analytical results on an industrial scale. The analyzed material was structural carbon steel. The tested material comprised steel manufactured in three different metallurgical processes. The resulting heats differed in purity and size of non-metallic inclusions. Heat treatments were selected to produce heats with different microstructure of steel, from hard microstructure of tempered martensite, through sorbitol to the ductile microstructure obtained by spheroidization. Pig iron accounted for approximately 25% of the charge. The study was performed on 21 heats produced in an industrial plant.

In the first process, steel was melted in a 140-ton basic arc furnace. The metal was tapped into a ladle, it was desulfurized and 7-ton ingots were uphill teemed. Billets with a square section of 100x100 mm were rolled with the use of conventional methods. As part of the second procedure, steel was additionally refined with argon after tapping into a ladle. Gas was introduced through a porous brick, and the procedure was completed in 8-10 minutes. Steel was poured into moulds, and billets were rolled similarly as in the first method. In the third process, steel was melted in a 100-ton oxygen converter and deoxidized by vacuum. Steel was cast continuously and square 100 x 100 mm billets were rolled with the use of conventional methods. Billet samples were collected to determine: chemical composition - the content of alloy constituents was estimated with the use of LECO analyzers an AFL FICA 31000 quantometer and conventional analytical methods, relative volume of non-metallic inclusions with the use of the extraction method, dimensions of impurities by inspecting metallographic specimens with the use of a Quantimet 720 video inspection microscope under 400x magnification. It was determined for a larger boundary value of 2 µm. The number of particles measuring 2 µm and smaller was the difference between the number of all inclusions determined by chemical extraction and the number of inclusions measured by the video method. Analytical calculations were performed on the assumption that the quotient of the number of particles on the surface divided by the area of that surface was equal to the quotient of the number of particles in volume divided by that volume [28].

The percentage of sulfur-based inclusions was below the value of error in determinations of the percentage of oxygen-based inclusions, therefore, sulfur-based inclusions were excluded from further analyses. The main focus of the analysis was on oxygen-based inclusions.

A total of 51 sections were examined to determine the fatigue strength of all heats. The analyzed sections had a cylindrical shape and a diameter of approximately 10 mm. Their main axes were oriented in the direction of processing. The sections were thermally processed to determine differences in their structural characteristics. They were hardened for 30 minutes from the austenitizing temperature of 880°C and quenched in water. The analyzed samples were tempered for 120 minutes at a temperature of 200, 300, 400, 500 or 600°C and cooled in air.

Fatigue strength was determined for all heats. Heat treatment was applied to evaluate the effect of hardening on the fatigue properties of the analyzed material, subject to the volume of fine non-metallic inclusions. The application of various heat treatment parameters led to the formation of different microstructures responsible for steel hardness values in the following range from 271 to 457 HV [21].

The test was performed on a rotary bending fatigue testing machine at 6000 rpm. The endurance (fatigue) limit was set at 10^7 cycles. The level of fatigue-inducing load was adapted to the strength properties of steel. Maximum load was set for steel tempered at a temperature of 200^0C - 650 MPa, from 300^0C to 500^0C - 600 MPa and for 600^0C - 540 MPa. During the test, the applied load was gradually reduced in steps of 40 MPa (to support the determinations within the endurance limit). Load values were selected to produce 10^4-10^6 cycles characterizing endurance limits [1].

The arithmetic average size proportions and distances between the impurities of structural steel α were calculated with the use of the below formula (8):

$$\omega = \frac{\bar{d}}{\bar{\lambda}} \tag{8}$$

where:
$\bar{d}$ – average diameter of impurity, µm;
$\bar{\lambda}$ - arithmetic average distance between impurities, µm.

The arithmetic average distances between impurities for each of the heats $\bar{\lambda}$ were calculated with the use of the below formula (9):

$$\bar{\lambda} = \frac{2}{3}\bar{d}\left(\frac{1}{V_0} - 1\right) \quad (9)$$

where:
$\bar{d}$ – average diameter of impurity, μm,
V_0 – relative volume of submicroscopic impurities, %.

The general form of the mathematical model is presented by equations (10) and (11)

$$k_{(tempering\ temperature)} = a\,\alpha + b \quad (10)$$

and

$$V_0 = g\,\alpha + h \quad (11)$$

where:
k - fatigue strength coefficient,
ω - arithmetic average size proportions and distances between impurities in structural steel,
V_0 - relative volume of non-metallic inclusions measuring 2 μm and smaller, vol. %.
a, b, g, h - coefficients of the equation

The significance of correlation coefficients r was determined based on the critical value of the Student's t-distribution for a significance level of α=0.05 and the number of degrees of freedom f = n-2 using formula (12).

$$t = \frac{r}{\sqrt{\frac{1-r^2}{n-2}}} \quad (12)$$

The values of diffusion coefficient z_{go} near the regression line were calculated with the use of the below formula (13):

$$\delta = 2s\sqrt{1-r^2} \quad (13)$$

where:
s – standard deviation,
r – correlation coefficient.

The values of the standard deviation s were calculated with the use of the below formula (14):

$$s = \sqrt{\frac{\sum(x-\bar{x})^2}{(n-1)}} \quad (14)$$

where:
x – result of measurement,
$\bar{x}$ – arithmetic average of measurement results.

3. Description of results

The chemical composition of the analyzed steel is presented in Table 1.

Fatigue strength coefficient k was calculated to determine the bending fatigue strength of hardened steel tempered at 200, 300, 400, 500 and 600°C subject to the quotient of the diameter of impurities and the spacing between impurities. The results are presented respectively in Figure 1-5. The regression equation and the value of the correlation coefficient r are shown respectively in (15)-(19).

$$k_{(200)} = 3.1407\ \omega + 0.6101 \text{ and } r = 0.8597 \quad (15)$$

$$k_{(300)} = 2.0141\ \omega + 0.68 \text{ and } r = 0.8158 \quad (16)$$

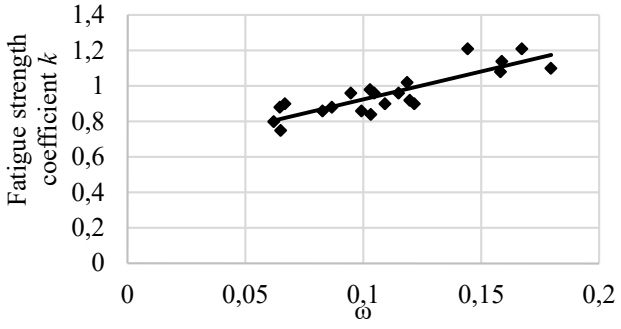

Fig. 1. Fatigue strength coefficient k of hardened steel tempered at 200°C subject the quotient of the diameter of impurities and the spacing between impurities ω

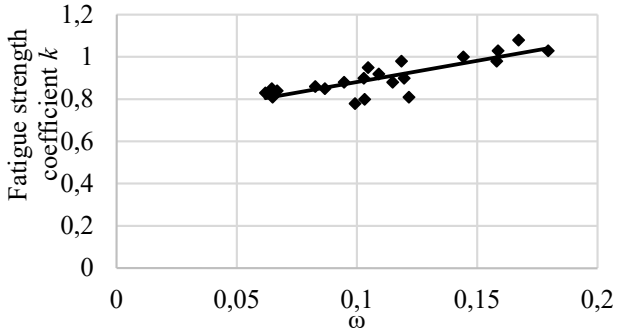

Fig. 2. Fatigue strength coefficient k of hardened steel tempered at 300°C subject the quotient of the diameter of impurities and the spacing between impurities ω

Table 1.
The chemical composition of the analyzed steel

C	Mn	Si	P	S	Cr	Ni	Mo	Cu	B
0.20-0.30	0.94-1.40	0.14-0.34	0.015-0.025	0.007-0.020	0.40-0.57	0.42-0.55	0.20-0.26	0.10-0.19	0.002-0.004

Table 2.
Parameters representing mathematical models (10 and 11) and correlation coefficients

Tempering temperature °C	Regression coefficient a (10) and g (11)	Regression coefficient b (10) and h (11)	Correlation coefficient r	Degree of dissipation k around regression line δ (14)	$t_{\alpha=0.05}$ calculated by (12)	$t_{\alpha=0.05}$ from Student's distribution for p=(n-2)
200	3.1407	0.6101	0.8597	55.1663	7.3362	2.093
300	2.0141	0.68	0.8158	34.7001	6.1487	
400	2.9667	0.5994	0.874	26.2400	7.8400	
500	1.9492	0.6796	0.8593	23.3231	7.3232	
600	2.4229	0.6581	0.8143	26.4683	6.1151	
All	2.4987	0.6454	0.8147	26.4427	6.1240	1.983

$$k_{(400)} = 2.9667\ \omega + 0.5994 \text{ and } r = 0.8740 \quad (17)$$

Fatigue strength coefficient k was calculated to determine the bending fatigue strength of hardened steel tempered at all analyzed temperatures subject to the quotient of the diameter of impurities and the spacing between impurities ω. The results are presented in Figure 6. The regression equation and the value of the correlation coefficient r are shown in (20).

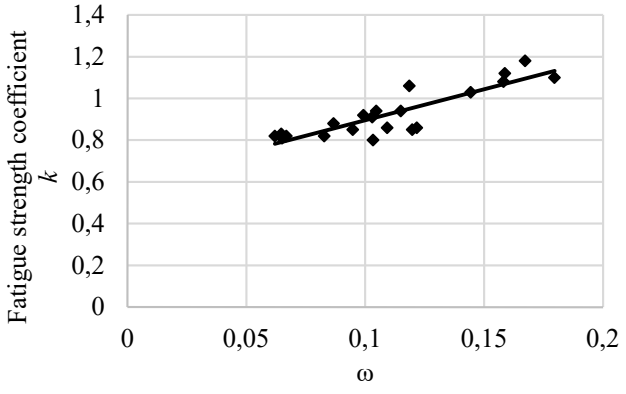

Fig. 3. Fatigue strength coefficient k of hardened steel tempered at 400°C subject the quotient of the diameter of impurities and the spacing between impurities ω

$$k_{(500)} = 1.9492\ \omega + 0.6796 \text{ and } r = 0.8593 \quad (18)$$

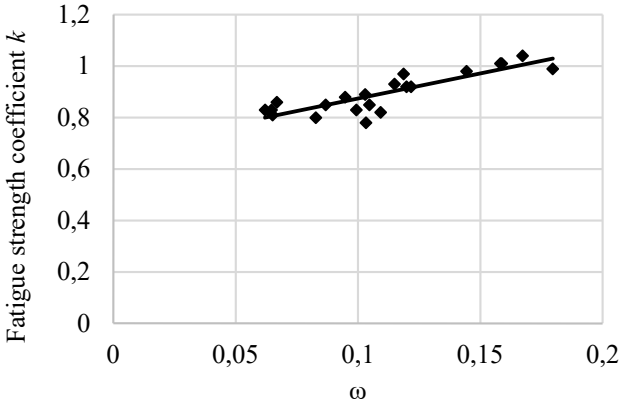

Fig. 4. Fatigue strength coefficient k of hardened steel tempered at 500°C subject the quotient of the diameter of impurities and the spacing between impurities ω

$$k_{(600)} = 2.4229\ \omega + 0.6581 \text{ and } r = 0.8143 \quad (19)$$

$$k = 2.4987\ \omega + 0.6454 \text{ and } r = 0.8147 \quad (20)$$

The quotient of the diameter of impurities and the spacing between impurities ω in steel subject to relative volume all range of non-metallic inclusions V are presented in Figure 7. The regression equation and the value of the correlation coefficient r are shown in (21).

$$V_0 = 0.6317\ \omega + 0.0129 \text{ and } r = 0.9554 \quad (21)$$

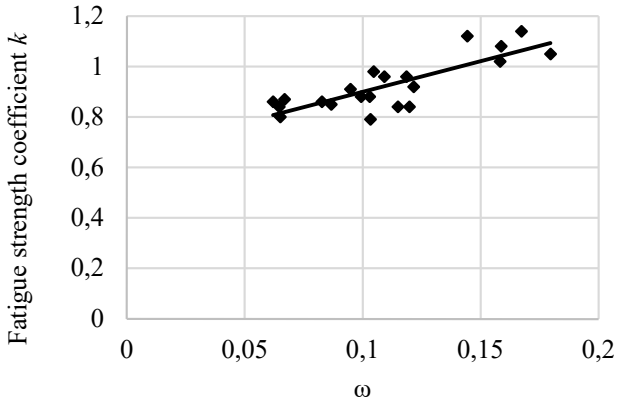

Figure 5. Fatigue strength coefficient k of hardened steel tempered at 600°C subject the quotient of the diameter of impurities and the spacing between impurities ω

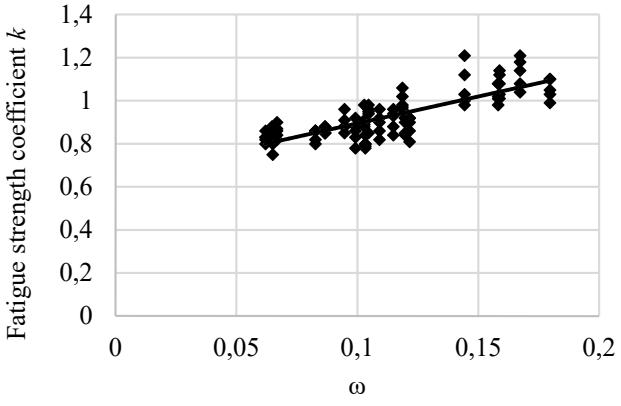

Fig. 6. Fatigue strength coefficient k of hardened steel tempered at all analyzed tempered temperatures subject to the quotient of the diameter of impurities and the spacing between impurities ω

In an analysis of regression equations (Table 3, Fig. 1-7) parameter a was determined in the range from 1.95 for tempering temperature 500°C to 3.14 for 200°C, and parameter b – in the range from 0.6 for 400°C to 0.68 for 300°C. Neither parameter was correlated with tempering temperature, correlation coefficient r or dissipation δ. All regression equations were characterized by a high correlation coefficient of over 0.81, which points to high statistical significance confirmed by Student's t-test. The above data indicate that the equations describing parameter k at different tempering temperatures, where r=0.815, can be replaced with a single equation for all tempering temperatures (22).

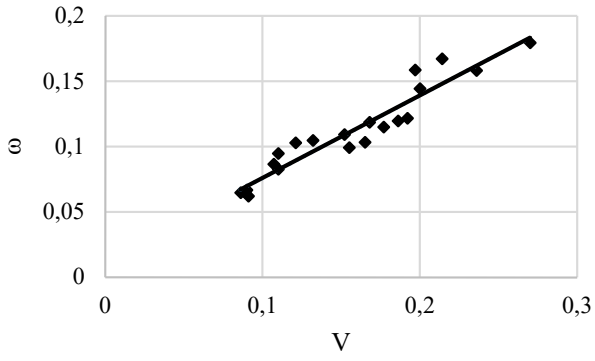

Fig. 7. The quotient of the diameter of impurities and the spacing between impurities ω in steel subject to relative volume all range of non-metallic inclusions V.

$$k = 2.5\omega + 0.65 \quad (22)$$

Based on (20), equation (22) can also be expressed as (23):

$$k = -3.96V + 0.7 \quad (23)$$

Based on (7) and (22), the relationship between the fatigue strength and hardness of high-grade steel under rotary bending conditions vs. the quotient of the diameter of impurities and the spacing between impurities (24) can be written as follows:

$$z_{go} = (2.5\omega + 0.65)HV \quad (24)$$

and based on (7) and (23), the relationship between the fatigue strength and hardness of steel vs. the relative volume of submicroscopic non-metallic inclusions can be written as (25):

$$z_{go} = (-3.96V + 0.7)HV \quad (25)$$

4. Conclusions

This study demonstrated correlations between the quotient of the diameter of impurities and the spacing between impurities, and the quotient of z_{go} and HV of non-metallic inclusions measuring at all range for high grade and high purity steels.

The proposed linear regression equations supported the determination of fatigue strength coefficient k with sufficient accuracy for every tempering temperature for high purity steels.

The proposed single equation for all tempering temperatures supports simpler calculation of parameters

k (22 and 23) and z_{go} (24 and 25), but with a somewhat greater error (Table 2).

To estimate fatigue strength based on the results of non-destructive tests, coefficient k was introduced in equations (24) and (25) to determine fatigue strength as a function of hardness.

Additional information

Selected issues related to this paper are planned to be presented at the 22nd Winter International Scientific Conference on Achievements in Mechanical and Materials Engineering Winter-AMME'2015 in the framework of the Bidisciplinary Occasional Scientific Session BOSS'2015 celebrating the 10th anniversary of the foundation of the Association of Computational Materials Science and Surface Engineering and the World Academy of Materials and Manufacturing Engineering and of the foundation of the Worldwide Journal of Achievements in Materials and Manufacturing Engineering.

References

[1] S. Kocańda, Fatigue failure of metals. WNT Warsaw 1985 (in Polish).

[2] D. Spriestersbach, P. Grad, E. Kerscher, Influence of different non-metallic inclusion types on the crack initiation in high-strength steels in the VHCF regime, International Journal of Fatigue 64 (2014) 114-120.

[3] S. Beretta, Y. Murakami, Largest-Extreme-Value distribution analysis of multiple inclusion types in determining steel cleanliness, Metallurgical and Materials Transactions 32B (2001) 517-523.

[4] J. Kloch, B. Billia, T. Okane, T. Umeda, W. Wołczyński, Experimental verification of the solute redistribution in cellular/dendritic solidification of the Al-3.5Li and Fe-4.34Ni Alloys, Materials Science Forum 329/330 (2000) 31-36.

[5] T. Himemiya, W. Wołczyński, Prediction of solidification path and solute redistribution of an iron-based multi-component alloy considering solute diffusion in the solid, Materials Transactions of the Japan Institute of Metals 43 (2002) 2890-2896.

[6] W. Wołczyński, E. Guzik, B. Kania, W. Wajda, interplay between temperature gradients field and c-e transformation in solidifying rolls, Archives of Foundry Engineering 9 (2009) 254.

[7] G.N. Kasatkin, Effect of nonmetallic inclusions on the mechanical properties of hydrogenated steels, Materials Science 40/6 (2004) 850-855.

[8] M. Faryna, W. Wołczyński, T. Okane, Microanalytical techniques applied to phase identification and measurement of solute redistribution at the solid/liquid interface of frozen Fe-4.3Ni doublets, Mikrochimica Acta, 139 (2002) 61-65.

[9] C.W. Anderson, G. Shi, H.V. Atkinson, C.M. Sellars, The precision of methods using the statistics of extremes for the estimation of the maximum size of inclusions in clean steels, Acta Materialia 48/17 (2000) 4235-4246.

[10] T. Lipiński, A. Wach, Influence of Outside Furnace Treatment on Purity Medium Carbon Steel. Proceedings of the 23rd International Conference on Metallurgy and Materials METAL 2014. TANGER Ltd., Ostrava, 2014, 738-743.

[11] L.A. Dobrzański, Heat treatment as the fundamental technological process of formation of structure and properties of the metallic engineering materials, Proceedings of the 8th Seminar of the International Federation for Heat Treatment and Surface Engineering IFHTSE, Dubrovnik-Cavtat, Croatia, 2001, 1-12.

[12] T. Lipiński, A. Wach, Dimensional structure of non-metallic inclusions in high-grade medium carbon steel melted in an electric furnace and subjected to desul-furization, Solid State Phenomena 223 (2015) 46-53.

[13] T. Lipiński, A. Wach, The effect of the production process and heat processing parameters on the fatigue strength of high-grade medium-carbon steel, Archives of Foundry Engineering 12/2 (2012) 55-60.

[14] L.A. Dobrzański, Synergic effects of the scientific cooperation in the field of materials and manufacturing engineering, Journal of Achievements in Materials and Manufacturing Engineering 15/1-2 (2006) 9-20.

[15] D. Podorska, P. Drożdż, J. Falkus, J. Wypartowicz, Calculations of oxide inclusions composition in the steel deoxidized with Mn, Si and Ti, European Materials Research Society, Warsaw University of Technology, 2006.

[16] W. Wołczyński, Back-Diffusion Phenomenon during the Crystal Growth by the Bridgman Method, Chapter 2, in: Modelling of Transport Phenomena in Crystal Growth, WIT Press, Southampton-Boston, 2000, 19-59.

[17] J.M. Zhanga, J.F Zhanga., Z.G. Yanga, G.Y. Lia, G. Yaoa, S.X. Lia, W.J. Huic, Y.Q. Weng, Estimation of maximum inclusion size and fatigue strength in high-strength ADF1 steel, Materials Science and Engineering A 394 (2005) 126-131.

[18] T. Cornelius, K. Birger, I. Nils-Gunnar, Fatigue anisotropy in cross-rolled, hardened medium carbon steel resulting from MnS inclusions, Metallurgical and Materials Transactions 37A (2006) 2995-3007.
[19] Y. Hai-Liang, L. Xiang-Hua, B. Hong-Yun, Ch. Li-Qing, J Deformation behavior of inclusions in stainless steel strips during multi-pass cold rolling, Journal of Materials Processing Technology 209 (2009) 455-461.
[20] Y. Murakami, Metal fatigue: Effects of small defects and inclusions, Amsterdam Elsevier, 2002.
[21] T. Lipiński, A. Wach, The effect of fine non-metallic inclusions on the fatigue strength of structural steel, Archives of Metallurgy and Materials 60/1 (2015) 65-69.
[22] Yu-Nan Wang, Jian Yang, Yan-Ping Bao, Effects of non-metallic inclusions on machinability of free-cutting steels investigated by nano-indentation measurements, Metallurgical and Materials Transactions A 46 (2015) 281-292.
[23] S.M. Mousavi, J. Paavola, Analysis of a cracked concrete containing an inclusion within homogeneously imperfect interface, Mechanics Research Communications 63 (2015) 1-5.
[24] T.Y. Shish, T. Araki, The effect of non-metallic inclusion and microstructures on the fatigue crack initiation and propagation in high strength carbon steel, Journal of ISIJ International 1 (1973) 11-19.
[25] J.S. Park J.H. Park, Effect of Slag Composition on the Concentration of Al_2O_3 in the Inclusions in Si-Mn-killed steel, Metallurgical and Materials Transactions 45B (2014) 953-960.
[26] S. Kocańda, J. Szala, Basis of fatigue calculation, PWN, Warsaw, 1985 (in Polish).
[27] Guide engineer. Mechanic. Scientific and Technical Publishing, Warsaw, 1970 (in Polish).
[28] J. Ryś, Stereology of materials, Fotobit Design, Cracow, 1995 (in Polish).